Engineering Computations

Finite element analysis of delamination of a composite component with the cohesive zone model technique

Luca Lampani

Received 21 October 2009
Revised 30 March 2010
Accepted 8 April 2010

Finite element analysis of delamination of a composite component with the cohesive zone model technique

Luca Lampani
Dipartimento di Ingegneria Aerospaziale e Astronautica, Università di Roma "La Sapienza", Roma, Italy

Abstract

Purpose – The purpose of this paper is to assess a numerical tool to simulate and predict the onset and the propagation of the delaminations in a composite structure.

Design/methodology/approach – The approach to the work is done through the cohesive zone model technique applied to the finite element method.

Findings – Double cantilever beam, end notched flexure and mixed mode bending tests have been performed and correlated to benchmark cases, in order to validate the procedure. Numerical test campaign on specimens of the skirts with delaminations has been performed to analyze the behaviour under compressive load and the buckling.

Originality/value – This tool is applied to the study of the behaviour of some components in carbon/epoxy composite of a space structure in which one or more delaminations are eventually present following impact damage or manufacturing process. The components in particular are the booster's skirts of a small class launcher, subjected to a compressive load.

Keywords Finite element analysis, Composite materials, Modelling, Failure (mechanical)

Paper type Research paper

1. Introduction

The increasing diffusion of the composite materials in the design of structures with high reliability requirements, as, i.e. in aeronautics and aerospace field, drives the study of problems inherent with this kind of materials. Inside this study, a relevant role is occupied from the damages induced through the delamination of laminated panels. The presence of a delamination might induce several failure mechanisms that sometimes combine buckling phenomena with delamination propagation, as described in Gaudenzi (1997) and Gaudenzi *et al.* (1998, 2001). In the present contribution, the attention is particularly focused on the possible onset of delamination propagation with reference to an application where a cylindrical composite component is considered. In order to provide an adequate prediction of the onset and propagation of this damage, some modeling techniques have been developed in last 30 years. Between them it is possible to

This work has been developed in the context of a research project of ESA/ESRIN, Vega Program, Directorate of Launchers, under the supervision of Dr Michel Bonnet awarded to the research group of Professor Paolo Gaudenzi of the Dipartimento di Ingegneria Aerospaziale e Astronautica of Università di Roma "La Sapienza". A special thank to Professor Paolo Gaudenzi for his continuous support in the development of the present work.

Engineering Computations: International Journal for Computer-Aided Engineering and Software
Vol. 28 No. 1, 2011
pp. 30-46

0264-4401
DOI 10.1108/02644401111097000

include the well known virtual crack closure technique (VCCT) (Krueger, 2004; Rybicki and Kanninen, 1977; Raju, 1987) and the more recent cohesive zone model (CZM) (de Borst, 2001, 2003). Both techniques can be implemented in a finite element analysis (Camanho *et al.*, 2001) for a versatile application.

Tuning a reliable methodology suitable for investigating about eventual delamination damages can be occur in a composite structural component from a design point of view has be done. In particular, the work founded a specific application in the verification of requirements of a small class launcher. The aim of this paper is to describe this work.

The VCCT is an approximate method that is derived from the more fundamental CCT and it is based on the Griffith crack growth criterion assuming a linear elastic fracture mechanics. In the CCT, according to the Irwin's assumption, when a crack extends by a small amount Δa the strain energy released in the process is equal to the work required to close the crack to its original length. This assumption holds true only, if Δa is small compared to the total crack length and self similar crack growth takes place, i.e. the shape of the crack does not change significantly during crack growth.

The VCCT is well suitable for elastic materials and when there is a small yielding zone around a sharp crack tip. For composites, the material non-linearity at the crack tip cannot be neglected. There exists a processing zone ahead of crack tip due to micro cracking, fiber bridging, coalescence of voids and other resources of micro level interactions. All these factors make the crack tip blunt and the VCCT not provides a satisfying model. CZM instead can take into account this damage zone (or material softening) that develops near the crack tip. For this reason the CZM has been chosen as most suitable technique for this work.

2. Cohesive zone model

The mechanical behaviour of composites is often strongly dependent of the crack propagation through the interface regions and then the toughness of a fiber composite is dependent both of the matrix-fiber interfaces and frictional sliding along the interfaces. For laminated composites the damage can also occur by delamination of the plies. Tensile strengths and energy dissipation play the main role in this kind of damage.

The energy-based fracture criteria are interested just by the toughness of the interface, whereas the strength-based fracture criteria are interested just by its strength. For a complete modeling of the delamination behaviour a full description of fracture that incorporates both types is mandatory. Cohesive-zone models for interfaces are defined both by strength and energy parameters that can be considered by modeling the tractions between interfaces. These tractions are representative of physical, chemical or mechanical bonding across a plane, or between two planes where an intermediate layer of resin is interposed. In this case it is possible to associate these tractions to the characteristic displacement that represents the failure strain of the cohesive zone. CZM can be implemented with FEA by using continuum type elements when the CZM is considered as a continuous compliant layer (Figure 1).

The cohesion elements have initially no-thickness. They connect the laminae of a composite laminate through their constitutive behaviours, expressed in terms of relative displacements and tractions across the interface (Beer, 1985).

The vector of the relative displacement in global coordinates, δ, can be obtained, as:

$$\delta = \sqrt{(u_1 - u_2)^2 + (v_1 - v_2)^2 (w_1 - w_2)^2} \tag{1}$$

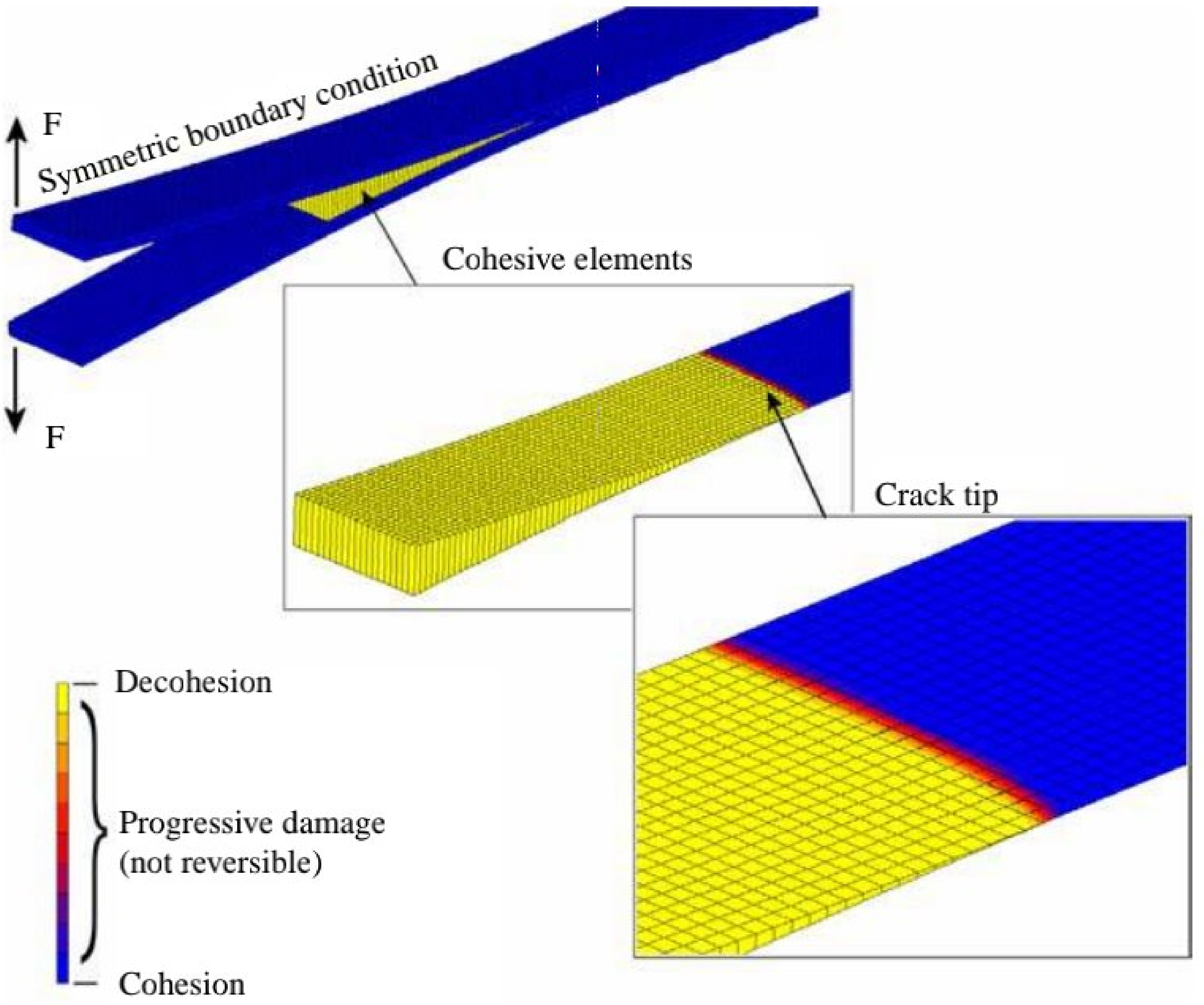

Figure 1.
Cohesive finite elements

where (u_1, v_1, w_1) and (u_2, v_2, w_2) are the global displacements for nodes 1 and 2 shown in Figure 2. The crack tip opening Δu, Δv and Δw are computed between nodes 1 and 2 in the global coordinate system and projected into the local coordinate system to obtain δ_I, δ_{II} and δ_{III}, corresponding to Modes I, II and III, respectively:

$$\delta = \sqrt{\delta_I^2 + \delta_{II}^2 + \delta_{III}^2} \tag{2}$$

Same procedure is applied to the local nodal forces F_I, F_{II} and F_{III} at the crack tip.

2.1 Constitutive decohesion model

Physically, the cohesive zone represents the coalescence of crazes in the resin rich layer located at the delamination tip and reflects the way by which the material loses load-carrying capacity.

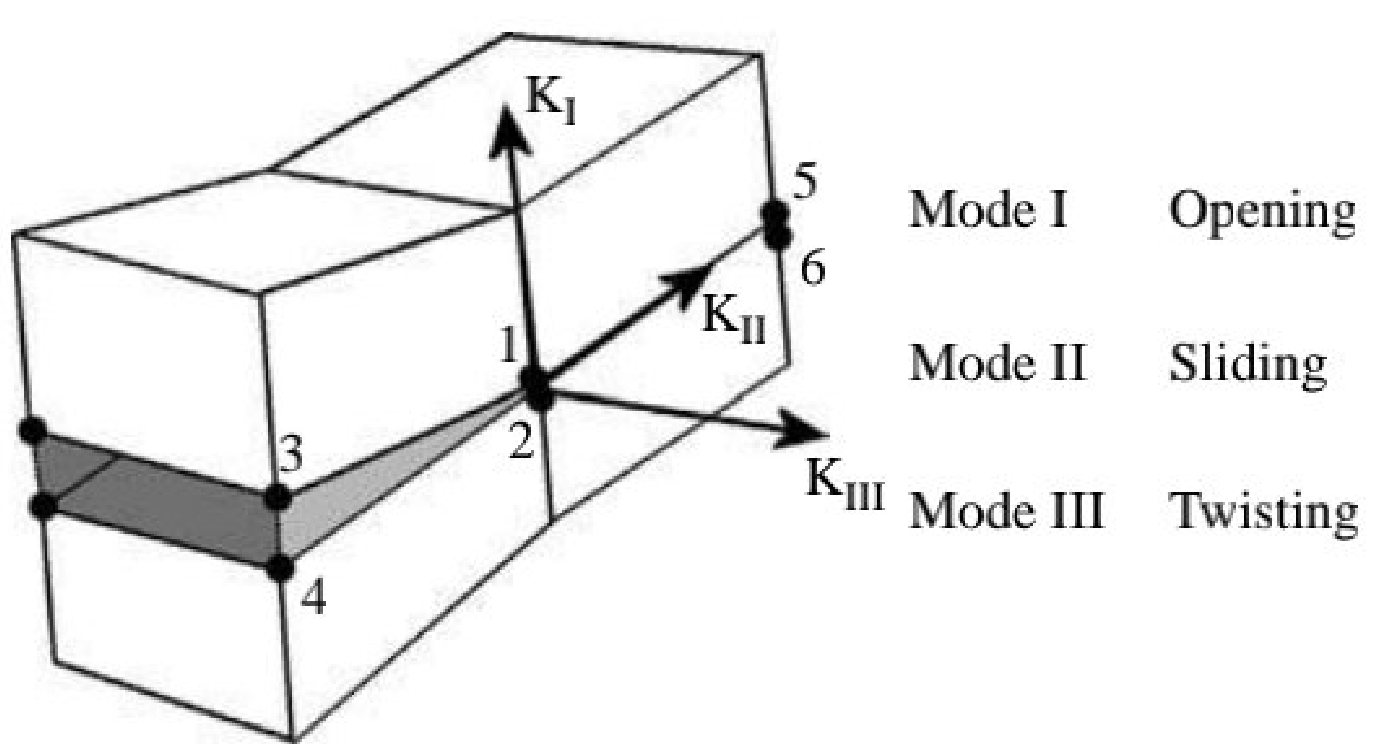

Figure 2.
Three modes decohesion across the interface

For pure Mode I and pure Modes II or III loading the bi-linear softening constitutive behaviour shown in Figure 3 and expressed in equations (3), (4) and (5) is used Camanho *et al.* (2003):

$$\sigma = \frac{2G_C}{\delta_{MAX}} \frac{\delta}{\delta_C} \quad if \quad 0 \le \delta \le \delta_C \tag{3}$$

$$\sigma = \frac{2G_C}{\delta_{MAX}} \left(\frac{\delta_{MAX} - \delta}{\delta_{MAX} - \delta_C} \right) \quad if \quad \delta_C \le \delta \le \delta_{MAX} \tag{4}$$

$$\sigma = 0 \quad if \quad \delta \ge \delta_{MAX} \tag{5}$$

For the segment of curve between (0, 0) and (δ_C, σ_{MAX}) the cohesion elements follow linear behaviour with a high initial stiffness (penalty stiffness, K). When the δ_C is never reached, in this range the behaviour is completely elastic and reversible. The cohesive layer deforms like an elastic material with the property of the resin. For pure Mode I, II or III loading, after the interfacial normal or shear tractions attain their respective interlaminar tensile or shear strengths (δ_C, σ_{MAX}) the behaviour changes in not-reversible and the stiffnesses are gradually reduced to zero. The elements have a permanent damage. The amount of this damage spans from a little decrease of the stiffnesses until the complete separation of the laminae ($\delta \ge \delta_{MAX}$). During this softening phase at each instant can be an unloading behaviour. In this case the curve unloads towards the origin, as shown in Figure 3 The area under the traction-relative displacement curves is the respective (Mode I, II or III) fracture toughness (G_{IC}, G_{IIC} and G_{IIIC}, respectively) and defines the final relative displacements, δ_{1MAX}, δ_{2MAX} and δ_{3MAX}, corresponding to complete decohesion. However, it is necessary to avoid the interpenetration of the crack faces. The contact problem is addressed by re-applying the normal penalty stiffness when interpenetration is detected.

2.2 CZM with FE

Stiffness of the CZM. The stiffness of the cohesive layer can contribute to the global deformation of the laminate but the only purpose of this kind of elements is to simulate the delamination. In order to obtain a good finite element model using CZM it is important that the stiffness of the cohesive elements, before the propagation of the delamination, is large enough to avoid the introduction of a fictitious compliance to the model Turon *et al.* (2007).

The whole laminate can be considered composed of two sublaminates connected by the cohesive layer Figure 4. The effective stiffness of the laminate can be calculated in the following way.

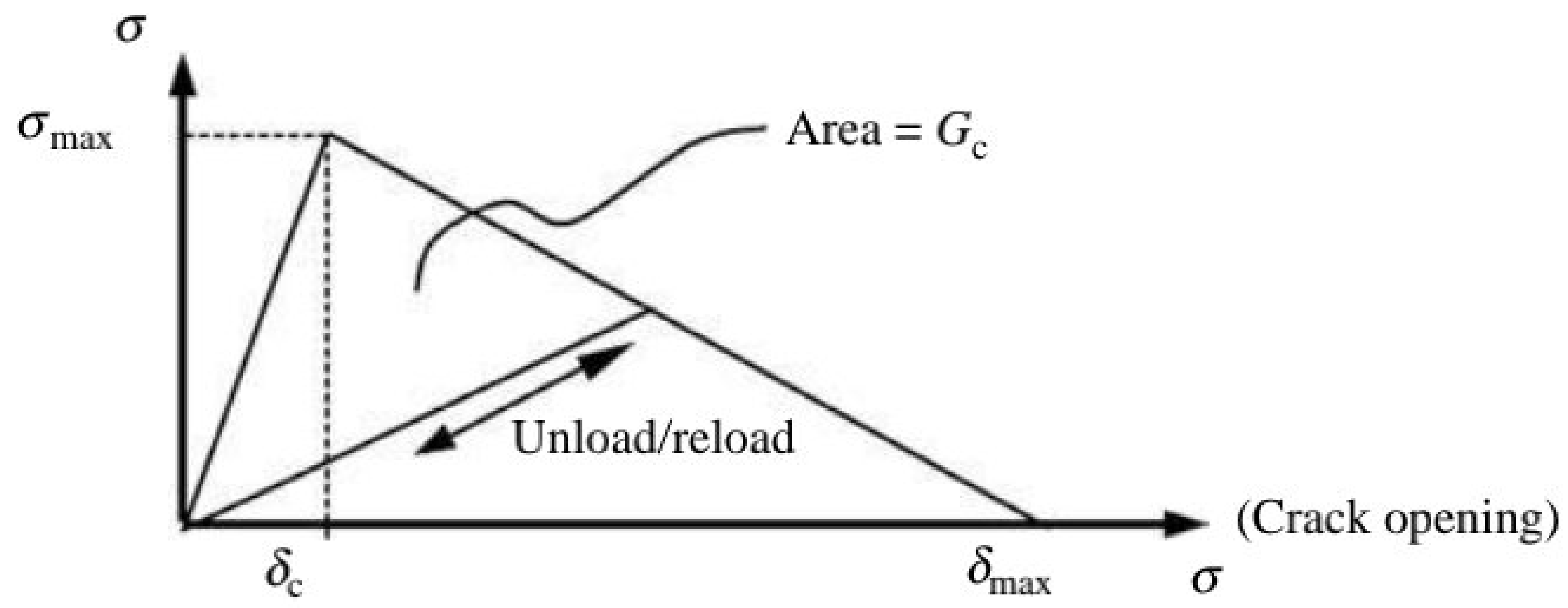

Figure 3.
Pure mode constitutive behaviour

Direction 3 is the through-the-thickness. For the stress along this direction it can be written:

$$\sigma = E_3 \varepsilon = K^I \delta \tag{6}$$

where ε is the transverse strain, K^I is the penalty stiffness for the first mode, δ its opening displacement and E_3 is the through-the-thickness Young's modulus of the material.

The effective strain of the composite is:

$$\varepsilon_{eff} = \frac{dt}{t} + \frac{\delta}{t} = \varepsilon + \frac{\delta}{t} \tag{7}$$

and the effective Young's modulus can be written as:

$$E_{eff} = E_3 \left(\frac{1}{1 + E_3 / K^I t} \right) \tag{8}$$

Penalty stiffness K^I proposed by Turon *et al.* (2007) can be calculated from equation:

$$K^I = \frac{\alpha E_3}{t} \tag{9}$$

For $\alpha > 50$ the loss of stiffness due to the presence of the interface is less than 2 per cent, which is sufficiently accurate for most problems.

Other authors have determined the value for the penalty stiffness as a function of the interfaces properties. Deauville *et al.* (1995) have considered the interface a resin reach zone of small thickness $t_{\text{interface}}$ and have proposed penalty stiffness defined as:

$$K^I = \frac{E_3}{t_{\text{interface}}} \quad K^{II} = \frac{2G_{13}}{t_{\text{interface}}} \quad K^{III} = \frac{2G_{23}}{t_{\text{interface}}} \tag{10}$$

where E_3, G_{13} and G_{23} are the elastic moduli of the resin rich zone.

In Appendix the development of the element stiffness matrix of the CZM element is discussed.

Length of the cohesive zone. Another important factor to obtain a good finite element model using CZM is that the cohesive element size must be less than the length of the cohesive zone l_{CZ}. This is defined as the distance from the crack tip to the point where the maximum cohesive traction is attained. The finite element spatial discretization has to be refined. If l_E is the mesh size in the region of the crack, we can express the number of elements in the cohesive zone as:

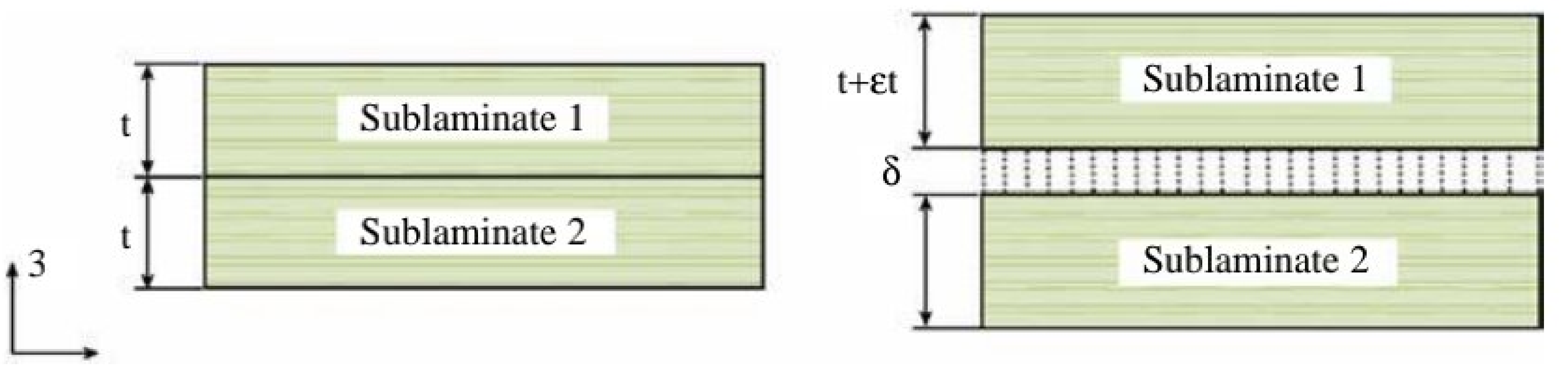

Figure 4.
Laminate with cohesive layer schematic model

$$N_E = \frac{l_{CZ}}{l_E} \quad (11)$$

When the cohesive zone is discretized by too few elements, the distribution of tractions ahead of the crack tip is not represented accurately. l_{CZ} is proposed from some authors in Table I.

A drawback in the use of CZM is that very fine meshes are needed to assure a reasonable number of elements in the cohesive zone. In order to go over this problem, some authors (Turon *et al.*, 2007; Alfano and Crisfield, 2001) developed a strategy to adapt the length of the cohesive zone to a given mesh size and to select opportunely the parameters of the interface with coarser meshes.

3. DCB, ENF and MMB tests

With the aim to validate the CZM theory applied to the finite element method as a tool for the analysis of propagation of the delaminations in composite material structures, three kind of benchmark cases (Dávila *et al.*, 2001; Harper and Hallett, 2008; Warrior *et al.*, 2003) are examined (Figure 5):

(1) Double cantilever beam (DCB) test, for decohesion Mode I.

(2) Three end notched flexure (3ENF) test, for decohesion Mode II.

(3) Mixed mode bending (MMB) test, for decohesion Modes I and II.

3.1 Finite element analyses of DCB and ENF tests

Under pure Modes I, II or III loading, the delamination propagation is predicted when the energy release rate (G_I, G_{II} or G_{III}) is equal the corresponding fracture toughness of the material (G_{IC}, G_{IIC} or G_{IIIC}):

$$G_i = G_{iC} \quad (12)$$

The pure modes can be studied through the DCB and ENF tests. In Figure 6, the geometrical dimensions of the specimen, used for both tests, are shown. The material and cohesive properties are reported in Table II. These are based on experimental data extracted from a unidirectional laminate of HTA/6376C composite, used in numerous delamination tests reported in literature (Borg *et al.*, 2004). The numerical results have been compared with the experimental ones.

Hui *et al.*	$\frac{2}{3\pi} E \frac{G_C}{\sigma_{MAX^2}}$
Irwin	$\frac{1}{\pi} E \frac{G_C}{\sigma_{MAX^2}}$
Dugdale, Barenblatt	$\frac{\pi}{8} E \frac{G_C}{\sigma_{MAX}}$
Rice, Falk *et al.*	$\frac{9\pi}{32} E \frac{G_C}{\sigma_{MAX^2}}$
Hillerborg *et al.*	$E \frac{G_C}{\sigma_{MAX^2}}$

Table I. Length of the cohesive zone

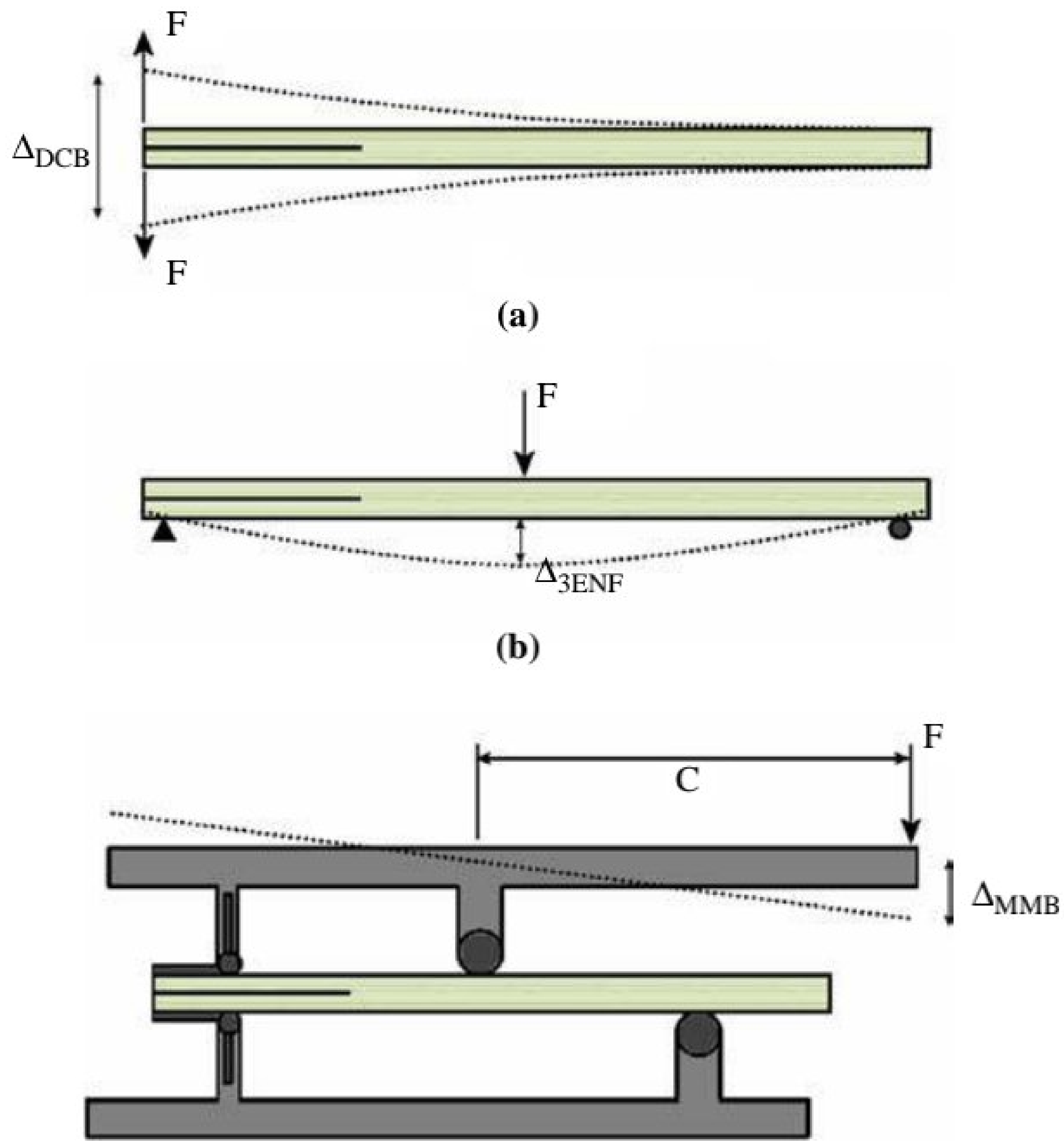

Figure 5.
DCB, 3ENF and MMB tests

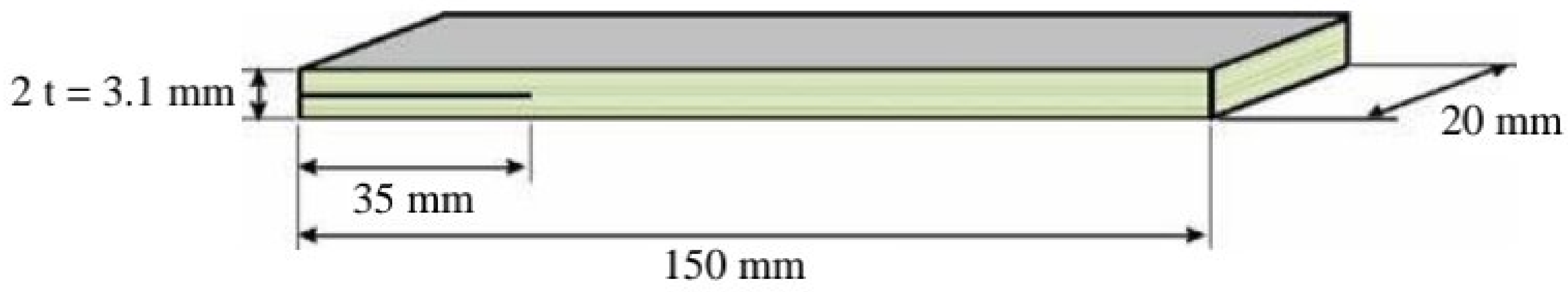

Figure 6.
Specimen dimensions for DCB and ENF tests

Table II.
Material properties for HTA6376/C

Layup	$[0_{12}//(\pm 5/0_4)_S]$
E_{11} (GPa)	120
$E_{22} = E_{33}$ (GPa)	11.5
$G_{12} = G_{13}$ (GPa)	5.25
G_{23} (GPa)	3.48
$\nu_{12} = \nu_{13}$	0.3
ν_{23}	0.51
G_{IC} (N/m)	260
G_{IIC} (N/m)	1,002
σ_{IMAX} (MPa)	30
σ_{IIMAX} (MPa)	60
K_I (N/mm^3)	1×10^6
K_{II} (N/mm^3)	1×10^6

The finite element models adopted for these studies are constituted of eight nodes solid hexahedral elements with zero initial thickness and governed by a bi-linear constitutive law for the cohesive ones. This was developed from a discrete interface element formulation, which has been successfully implemented to model both matrix cracking and delamination within notched composites using the finite element code Marc with implicit scheme. The composite material elements are eight nodes solid hexahedral with an orthotropic material model. The experimental and numerical analyses are performed under quasi-static loading conditions. With a velocity of the prescribed displacements in the order of mm/min in order to minimize the effects of the dynamics, the crack propagates more gradually and with small oscillations. The rate of the applied load is sufficiently small to induce a kinetic energy 0.25 per cent of the internal energy. An implicit time integration scheme is adopted for the FE analysis. Low loading rate would render the problem insolvable with an explicit FE method due to the inherent time step limitations. A mesh refinement from 1.25 mm down to 0.5 mm size assures the convergence of the analysis. The results of these tests are shown in Figures 7 and 8.

3.2 Finite element analyses of MMB test

The MMB test (Camanho *et al.*, 2003; Warrior *et al.*, 2003; Reeder and Crews, 1990; Tenchev and Falzon, 2007) is a combination of DCB and ENF tests. A loading lever presses the specimen in the middle to produce a bending and consequently shear stress component. The lever is also connected by a hinge to one end of the specimen, where an initial delamination, *a* long, is present to open the crack with Mode I. To obtain different values for the G_{II}/G_I mixed-mode delamination ratio for a unidirectional fiber composite specimen it is necessary to change the loading position c (Figure 5c). Pure Mode II loading occurs when the applied load is directly above the center of the specimen (c = 0). Pure Mode I loading can be achieved by removing the beam and pulling up on the hinge.

The failure criterion for delamination propagation in mixed mode can be expressed as:

$$f_{PROPAGATION} = f(G_i) - 1 = 0 \tag{13}$$

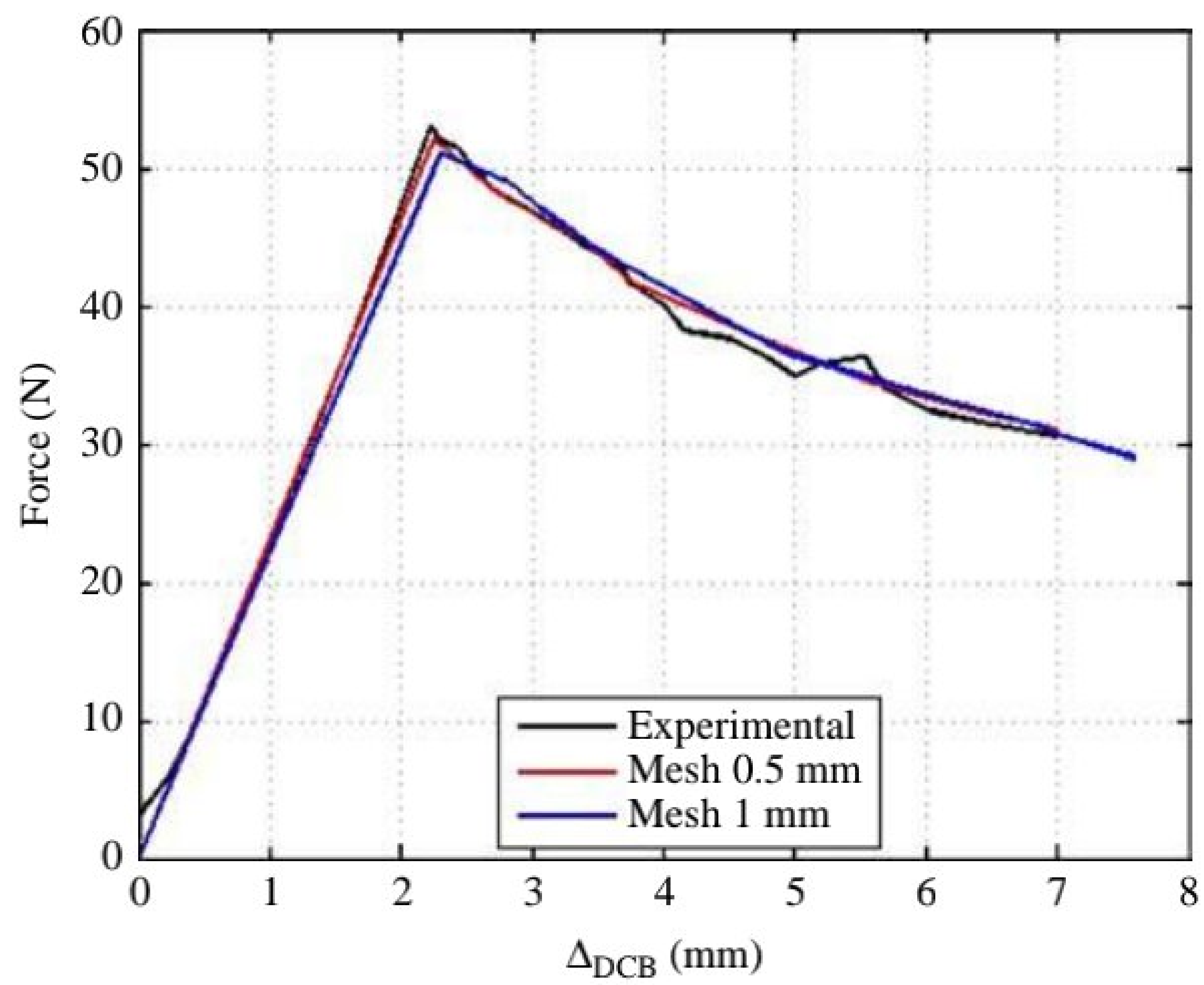

Figure 7. DCB test, numerical-experimental comparison

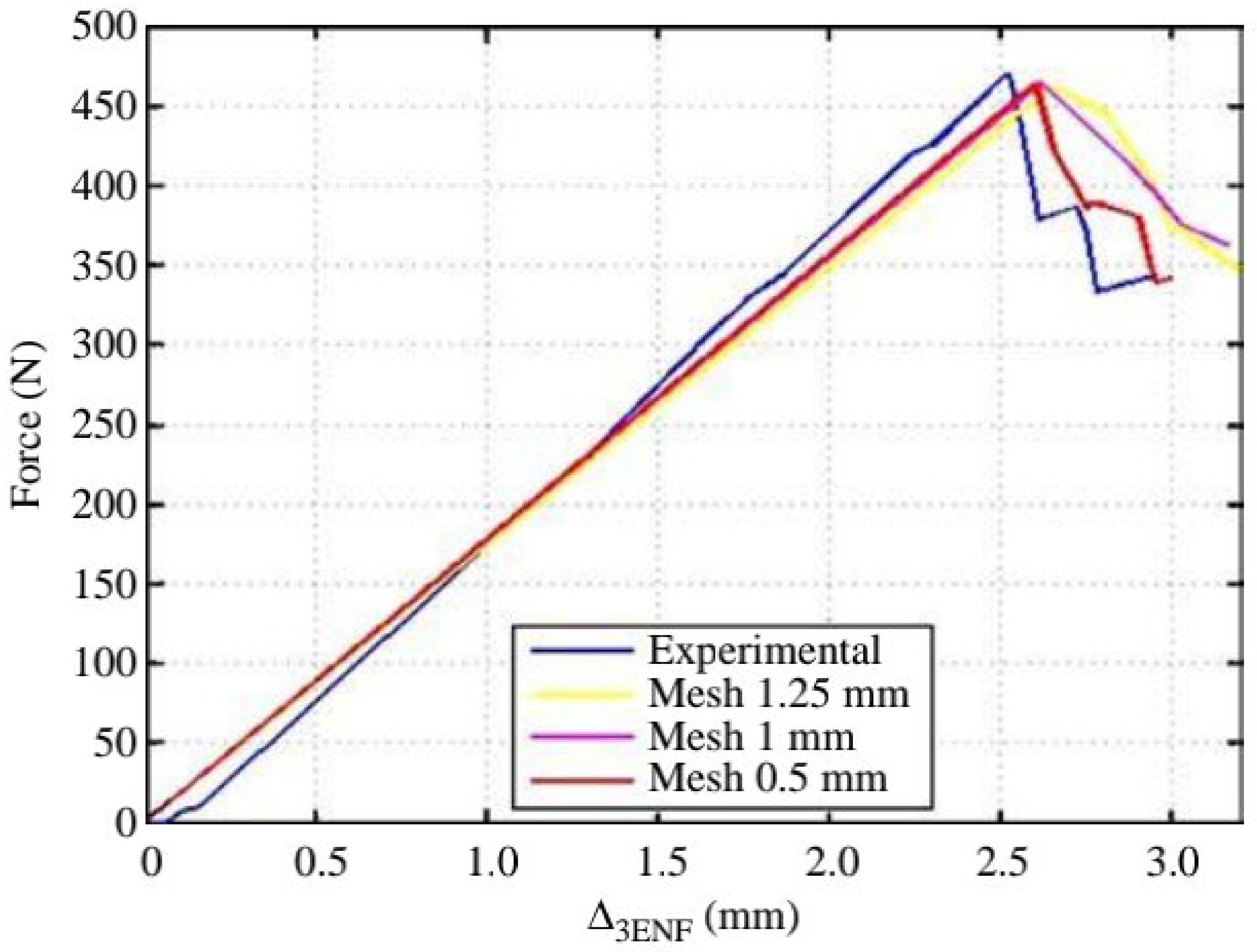

Figure 8.
3ENF test, numerical-experimental comparison

where $f_{PROPAGATION}$ is a function of the pure mode fracture energies and $f(G_i)$ is a norm of the energy release rates. One of the propagation criteria adopted in the literature is the power law expression:

$$f_{PROPAGATION}(G_i) = \left(\frac{G_I}{G_{IC}}\right)^{\alpha} + \left(\frac{G_{II}}{G_{IIC}}\right)^{\beta} + \left(\frac{G_{III}}{G_{IIIC}}\right)^{\gamma} - 1 = 0 \tag{14}$$

where α, β and γ are parameters to be fit with experimental data. The values $\alpha = \beta = \gamma = 1$ or $\alpha = \beta = \gamma = 2$ are frequently chosen when no experimental data is available.

For mixed-modes I and II, the MMB test is normally used. However, further research is required to assess the Mode III interlaminar fracture toughness, G_c^{III}. Some test methods have been suggested for the measurement of it, such as the edge crack torsion. There is an important parameter required for the analysis, the transverse shear modulus G_{23}. Furthermore, there is no reliable mixed-mode delamination failure criterion incorporating Mode III because there is no mixed-mode test method available incorporating Mode III loading. Therefore, most of the failure criteria proposed for delamination growth were established for mixed-modes I and II loading only. For these reasons the concept of energy release rate related with shear loading, $G_{shear} = G_{II} + G_{III}$, is used here. In these simulations identical data are used for both the modes II and III inputs to the CZM.

Benzeggagh and Kenane proposed a different criterion (B-K criterion) suitable for composite with epoxy matrix to accurately account for the variation of fracture toughness as a function of mode through a parameter η obtained from MMB tests at different mode ratios:

$$f_{PROPAGATION} = \frac{G_T}{G_C} - 1 = 0 \tag{15}$$

where G_T is:

$$G_T = G_I + G_{shear} \tag{16}$$

and G_C is:

$$G_C = G_{I\,C} + (G_{II\,C} - G_{I\,C})\left(\frac{G_{shear}}{G_T}\right)^{\eta} \quad (17)$$

Differently from the specimens used for the past two kind of tests, for the mixed one we adopted an unidirectional AS4/PEEK carbon-fiber reinforced composite specimen 102 mm long, 25.4 mm wide, 3.12 mm thick. The material properties for are resumed in Table III.

The results of these tests are shown in Figure 9 for a model with mesh size of 0.5 mm. Two different mixed-mode ratios, 50 and 80 per cent, are considered. For the first one the arm c is taken of 44.4 mm and the initial delamination length a of 34.1 mm. For the second c is 28.4 mm and a is 31.4 mm.

Layup	$[0_{24}]$
E_{11} (GPa)	122.7
$E_{22} = E_{33}$ (GPa)	10.1
$G_{12} = G_{13}$ (GPa)	5.5
G_{23} (GPa)	3.7
$\nu_{12} = \nu_{13}$	0.25
ν_{23}	0.45
G_{IC} (N/m)	969
G_{IIC} (N/m)	1,719
σ_{IMAX} (MPa)	80
σ_{IIMAX} (MPa)	100
K_I (N/mm^3)	1×10^6
K_{II} (N/mm^3)	1×10^6

Table III. Material properties for AS4/PEEK

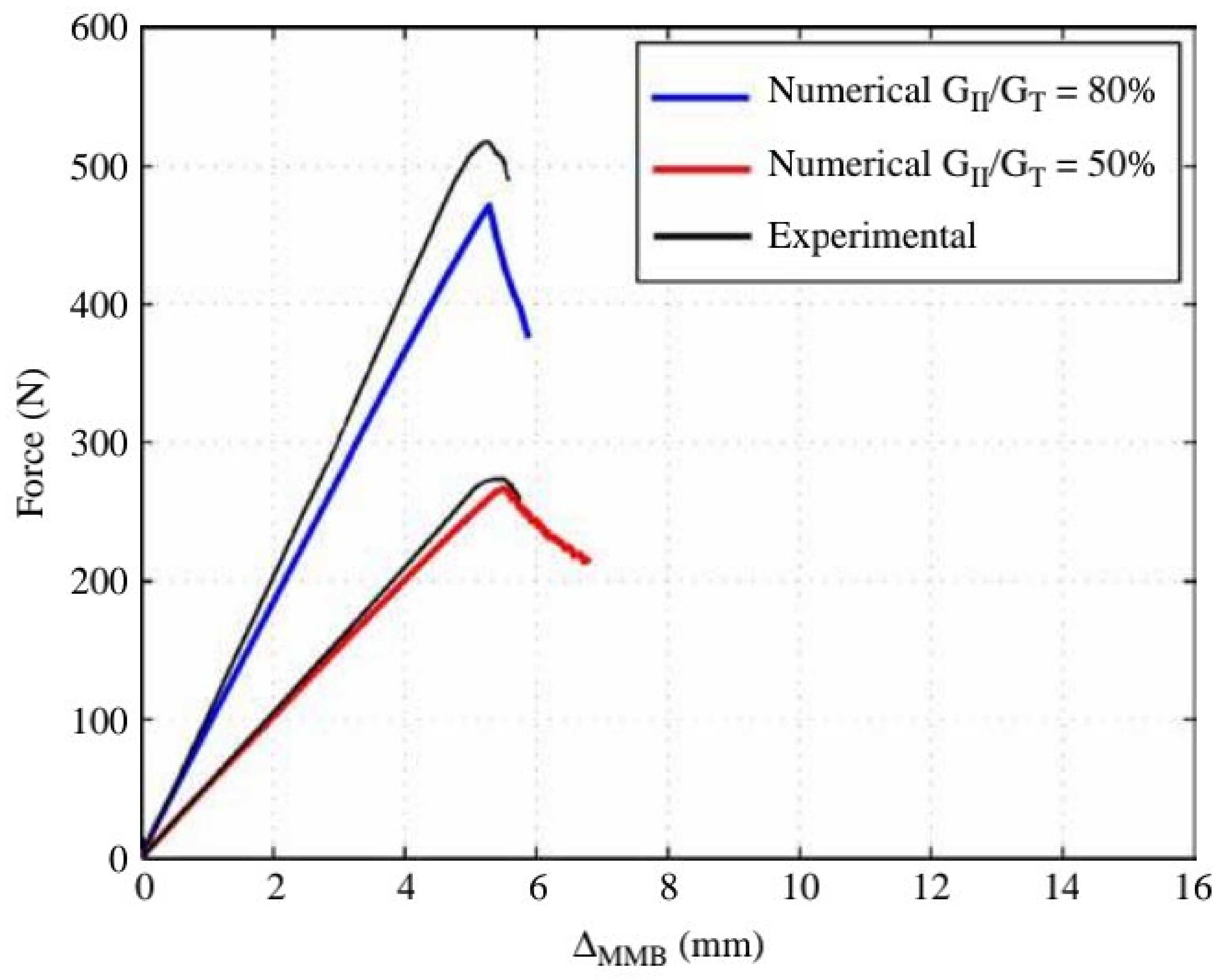

Figure 9. MMB test, numerical-experimental comparison

4. Delamination analysis of a booster's skirt

After the preparatory work to validate the method through the benchmarks, the efforts are concentrated on a topic application as the booster's skirt (Figure 10) of a small class launcher. The aim is to examine the behaviour of such a structure when a delamination inside the stacking sequence of the composite material is present. This delamination, present as manufacturing defect or as damage by impact, can have a stable or instable behaviour depending on the kind of load acting on the structure, that is the difference between propagate or not.

The structure, cylindrical shaped, is mainly subjected to axial compression. Under such a load some global, local (Bolotin, 2001) or mixed buckling condition can arise. Each of these conditions can take part in a more or less important amount in the evolution of the delamination. The grow in dimension of the delamination affects in turn the stiffness of the structure itself increasing the risk of buckling and then decreasing the value of the critical load. Moreover, the progression of a delamination is a non-reversible phenomena and the threshold of the critical load has to be updated in negative depending on the history of the load itself.

The CZM introduces non-linearity in the process because of its constitutive behaviour displacement dependent. The element stiffness matrix has to be updated on the basis of the history of the maximum displacements δ_i^* locally reached. Non-linear constitutive behaviour can be limited to the small region of the interface where the crack propagates, while the remaining part of the structure is often modeled as linear elastic. When further non-linearities are introduced in the finite element model, as when geometric non-linearity is taken into account (i.e. buckling analysis), non-linear stiffness terms are added in element stiffness of the composite solid elements. It is not the same for the cohesive elements that are affected anyway from large displacements of the interfaces.

One of the purposes of this work is to establish a relationship between the amount of the load and the progression of the delamination as well as the way of evolution, to understand the modality of failure for the structure. In order to know the condition of worse criticality for the evolution of the damage it need to perform a parametric analysis. The parameters are the depth in thickness of the delamination and the change in orientation of the plies as well as the initial shape and dimensions.

Such a kind of analysis is complex for the high number of tests and it is out of the purpose of the present work. Our effort is for the moment concentrated on few cases, performed on specimens of skirt instead of the whole one. Nevertheless, it is possible to extrapolate some interesting behaviour.

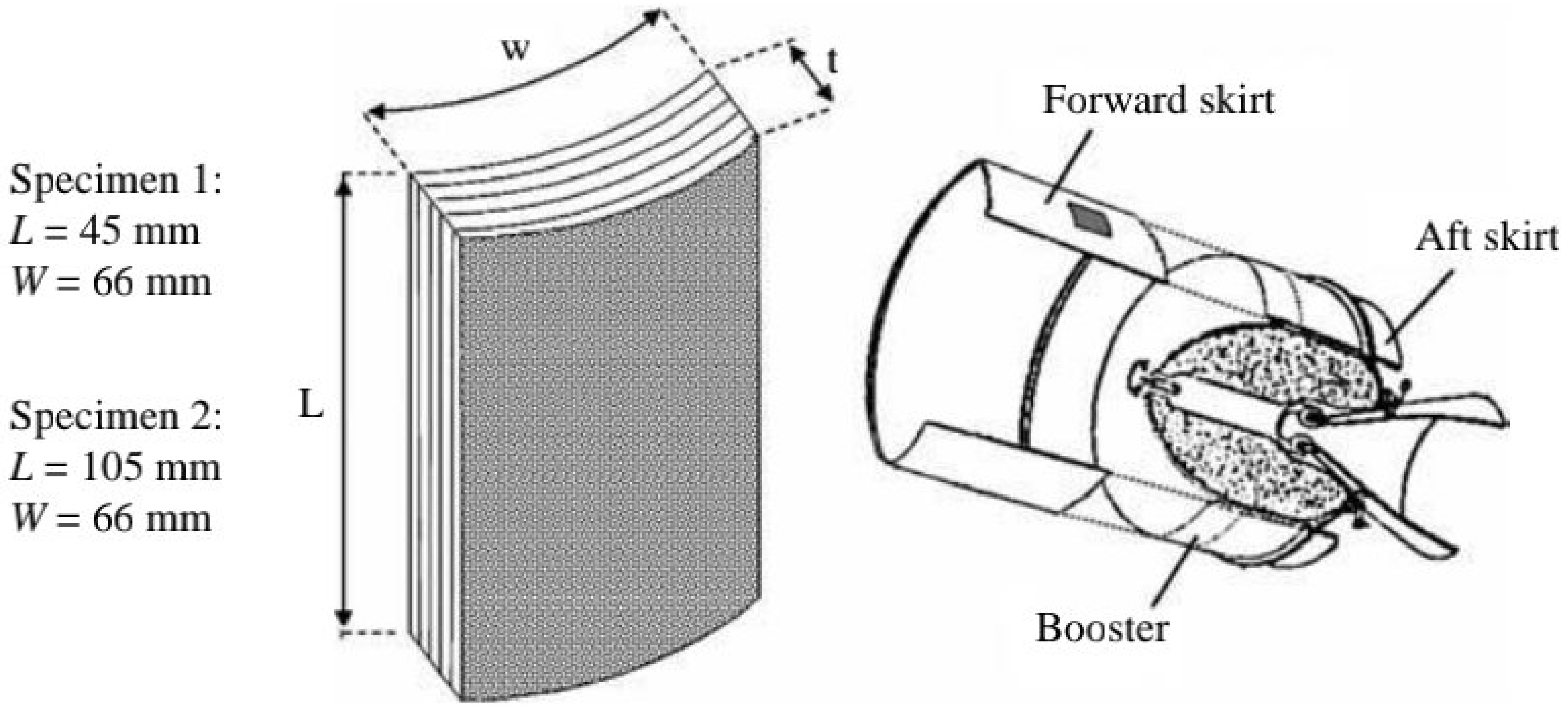

Figure 10.
Skirt's specimens

4.1 Finite element analyses of skirt's specimens

The reference skirt is made in carbon/epoxy material with properties reported in Table IV. The stratification sequence is composed of 55 plies oriented at 0°, ± 45° and 90° respect to the cylinder axis for a total thickness of about 8 mm. The diameter of the skirt is about 3 m.

The case of a delamination, circular shaped, with two different radii of 20 and 25 mm, between the 13th and the 14th layer (0°/90°) from the external surface, is considered. The numerical analyses are performed on two specimens extracted from the whole skirt. The dimensions are shown in Figure 10.

The finite element model (Figure 11) is composed of two sublaminates of eight nodes 3D composite elements, jointed by a layer of cohesive elements without initial thickness, with the exception of the initial delaminated region. In order to start an out-of-plane displacement of the delaminated region it is necessary to introduce an initial imperfection.

E_{11} (GPa)	153
E_{22} (GPa)	6.9
E_{33} (GPa)	6.9
G_{12} (GPa)	4.9
G_{23} (GPa)	4.9
G_{13} (GPa)	3.425
ν_{12}	0.34
ν_{23}	0.3
ν_{13}	0.0178
G_{IC} (N/m)	151
G_{IIC} (N/m)	690

Table IV. Reference skirt carbon/epoxy material properties

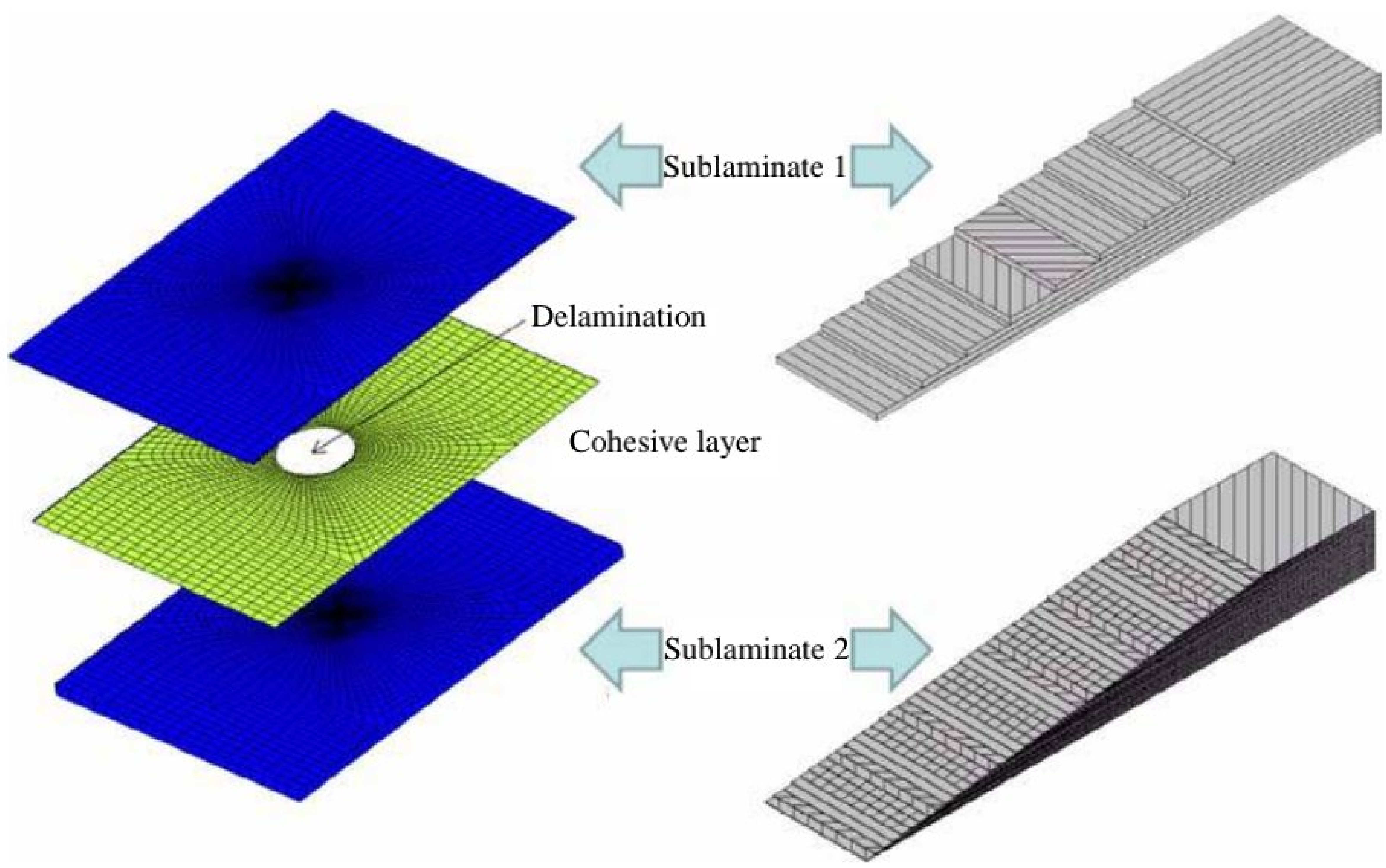

Figure 11. FE model of a skirt's specimen

This imperfection, sine shaped, represents the air bubble entrapped between the two sublaminates.

Despite the very little geometric ratio width-of-specimens/diameter-of-skirt, the FE models reproduce the curvature anyway. The capability of model curved structures is an important feature of the tool.

Figures 12 and 13 show the results of the compression tests on skirt's specimens type 1 and 2 for two different initial radii. On the *x*-axis the ratio between the progression of

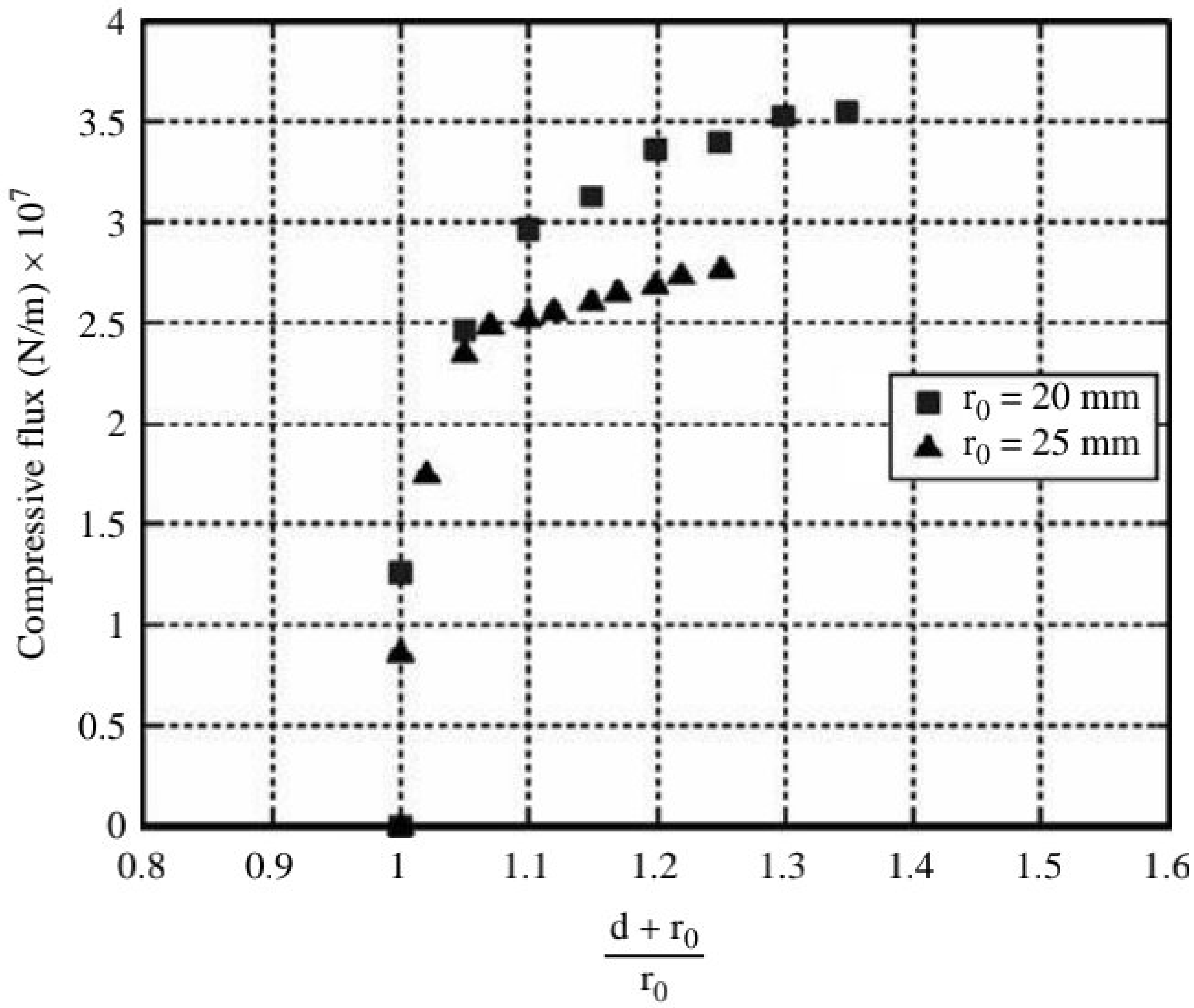

Figure 12.
Damage evolution graph for type 1 specimen

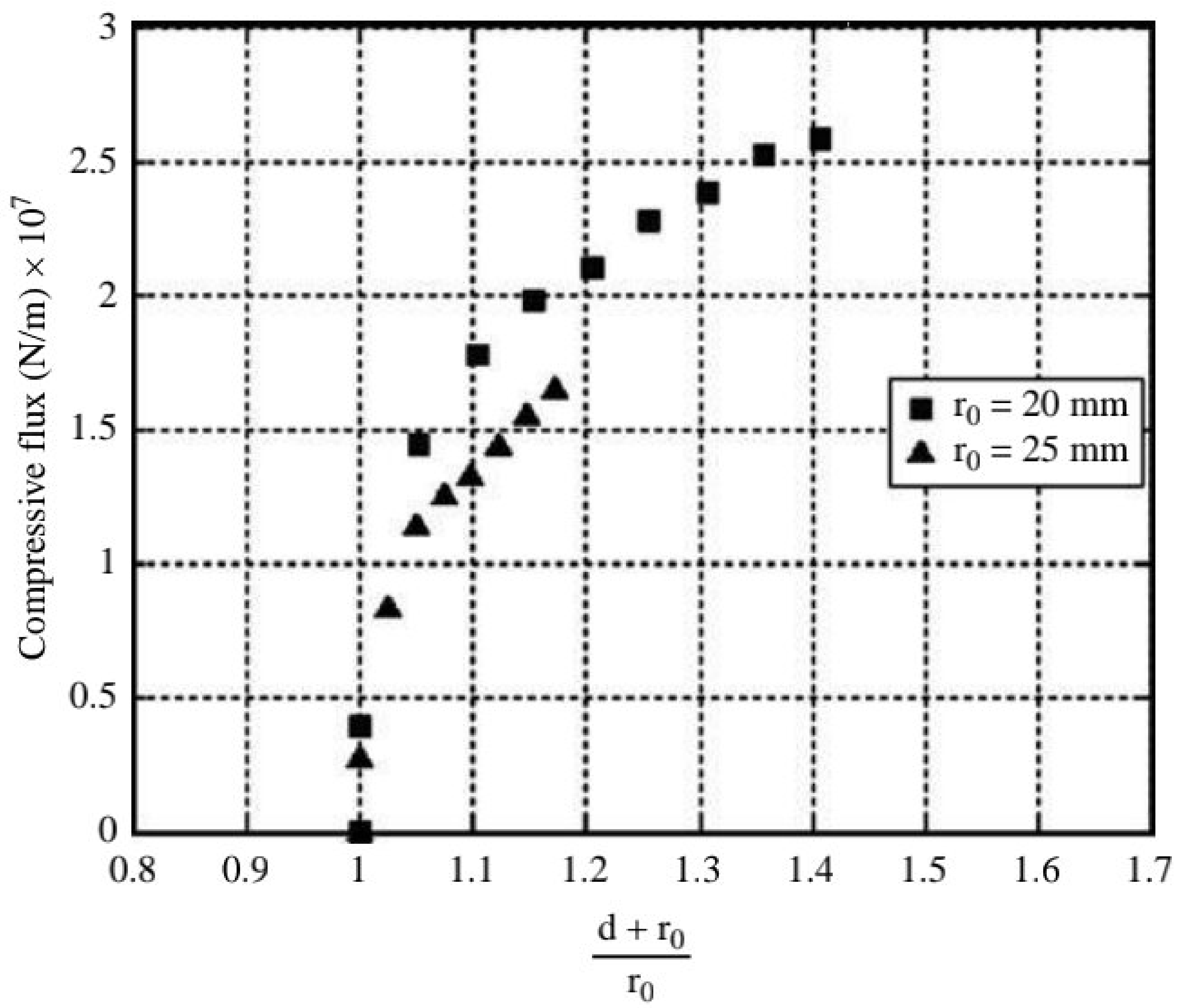

Figure 13.
Damage evolution graph for type 2 specimen

the delamination in circumferential direction and the initial radius is represented. On the *y*-axis the compressive flux on the skirt. The propagation front (Figure 14) is mainly direct in circumferential direction. The load necessary to propagate the damage have to increase less with the growing of the dimensions of the damage itself. This behaviour is also linked to the presence of a local buckling (Figure 15). Above a critical threshold, the delamination interests the whole circumference. From graphs can be also observed as the damage propagation is strongly affected by its initial dimensions.

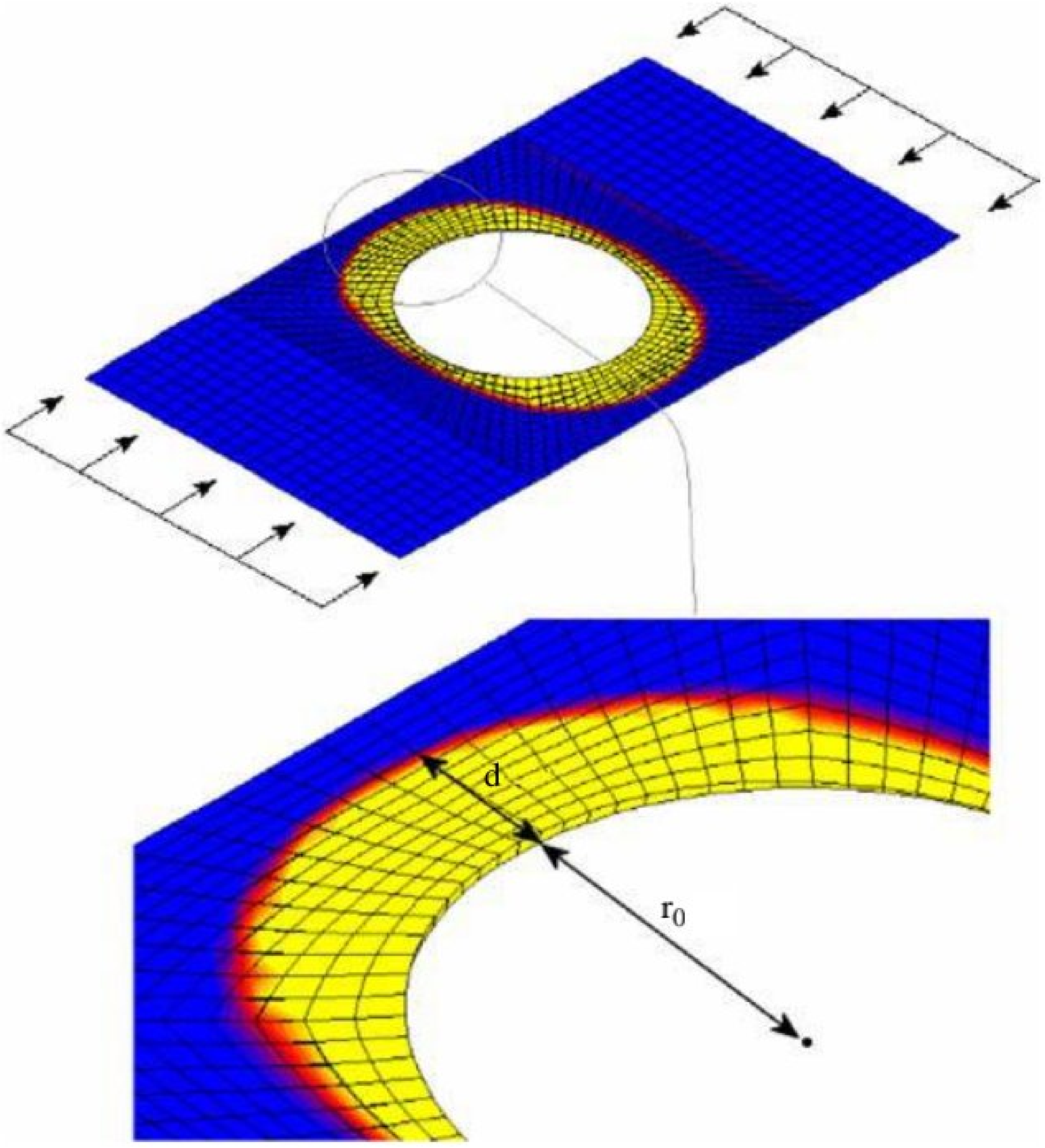

Figure 14. Damage evolution band plot (cohesive layer)

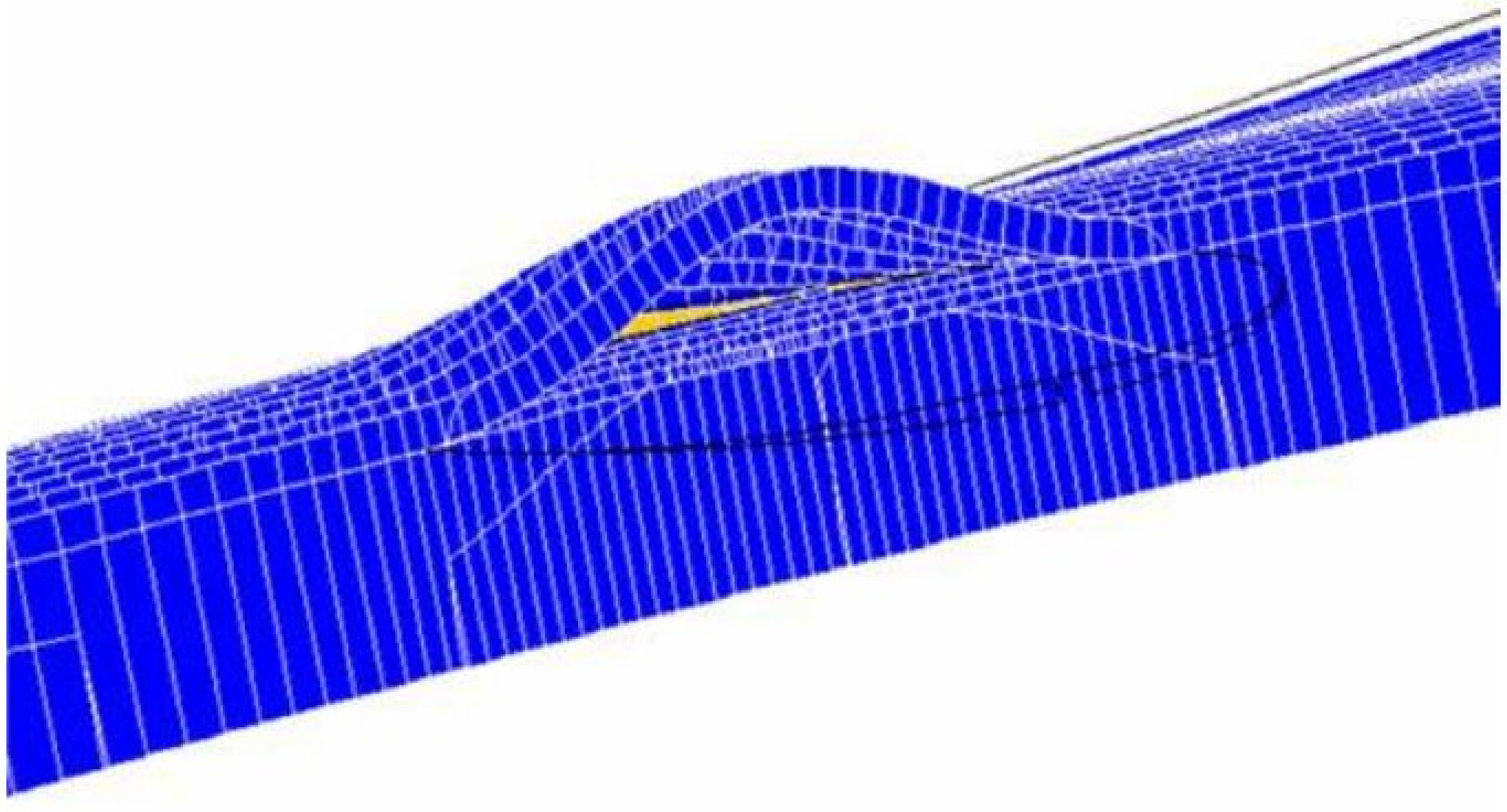

Figure 15. Local buckling effect

Conclusions

In this work, the CZM technique has been analyzed as tool to estimate the onset and propagation of a delamination in composite materials in the framework of the finite element numerical modeling. Through such a technique we succeeded in foreseeing the progression of a delamination in the booster's skirt of a small class launcher when it is solicited to axial compression loads. The assessment of this tool has been done with a campaign of validation by three kind of benchmark test, DCB, ENF and MMB, with a good correlation with experimental data.

In order to define a correct methodology and a very refined FEM procedure to predict a delamination emergence in laminate composite components it is anyway necessary to support the CZM method with approach strength based. The prediction of local interface failure which, can be considered as the onset of the formation of a delamination, can be evaluated with methods based on the computation of the interface strength. In laminated composites quadratic strength criteria, as, i.e. Tsai or Puck, are used successfully for this purpose. A first ply failure criterion is employed to predict delamination initiation, while delamination propagation is analyzed using an energetic approach for the fracture mechanics. The combination of an initiation criterion and a propagation criterion allows for a conservative estimation of the size and the location of the critical initial delamination, the delamination load, and the load carrying capacity of the structure.

References

Alfano, G. and Crisfield, M. (2001), "Finite element interface models for the delamination analysis of laminated composites: mechanical and computational issues", *International Journal for Numerical Methods in Engineering*, Vol. 77 No. 2, pp. 111-70.

Beer, G. (1985), "An isoparametric joint/interface element for finite element analysis", *International Journal for Numerical Methods in Engineering*, Vol. 21, pp. 585-600.

Bolotin, V.V. (2001), "Mechanics of delaminations in laminate composite structures", *Mechanics of Composite Materials*, Vol. 37 Nos 5/6.

Borg, R., Nilsson, L. and Simonsson, K. (2004), "Simulating DCB, ENF and MMB experiments using shell elements and a cohesive zone model", *Composites Science and Technology*, Vol. 64, pp. 269-78.

Camanho, P.P., Davila, C.G. and Ambur, D.R. (2001), "Numerical simulation of delamination growth in composite materials", NASA/TP-2001-211041, NASA Technical Publication, National Technical Information Service (NTIS), August.

Camanho, P.P., Davila, C.G. and de Mourra, M.F. (2003), "Numerical simulation of mixed-mode progressive delamination in composite materials", *Journal of Composite Materials*, Vol. 37 No. 16, pp. 1415-38.

Dávila, C.G., Camanho, P.P. and de Mourra, M.F. (2001), "Mixed-mode decohesion elements for analyses of progressive delamination", *Proceedings of the 42nd AIAA/ASME/ASCE/AHS/ASC Structures, Structural Dynamics and Materials Conference, Seattle, Washington, April 2001, AIAA-01-1486.*

Deauville, L., Allix, O. and Ladevèze, P. (1995), "Delamination analysis by damage mechanics: some applications", *Composite Engineering*, Vol. 5 No. 1, pp. 17-24.

de Borst, R. (2001), "Some recent issues in computational failure mechanics", *International Journal for Numerical Methods in Engineering*, Vol. 52, pp. 63-95.

de Borst, R. (2003), "Numerical aspects of cohesive-zone models", *Engineering Fracture Mechanics*, Vol. 70, pp. 1743-57.

Gaudenzi, P. (1997), "On delamination buckling of composite laminates under compressive loading", *Composite Structures*, Vol. 39 Nos 1-2, pp. 21-30.

Gaudenzi, P., Perugini, P. and Spadaccia, F. (1998), "Post-buckling analysis of a delaminated composite plate under compression", *Composite Structures*, Vol. 40 Nos 3-4, pp. 231-8.

Gaudenzi, P., Perugini, P. and Riccio, A. (2001), "Post-buckling behavior of composite panels in the presence of unstable delaminations", *Composite Structures*, Vol. 51, pp. 301-9.

Harper, P.W. and Hallett, S.R. (2008), "Cohesive zone length in numerical simulations of composite delamination", *Engineering Fracture Mechanics*, Vol. 75, pp. 4774-92.

Krueger, R. (2004), "Virtual crack closure technique: history, approach, and applications", *Applied Mechanics Reviews*, Vol. 57 No. 2.

Raju, I.S. (1987), "Calculation of strain-energy release rates with higher order and singular finite elements", *Engineering Fracture Mechanics*, Vol. 28, pp. 251-74.

Reeder, J.R. and Crews, J.R. Jr (1990), "Mixed-mode bending method for delamination testing", *AIAA Journal*, Vol. 28 No. 7, pp. 1270-6.

Rybicki, E.F. and Kanninen, M.F. (1977), "A finite element calculation of stress intensity factors by a modified crack closure integral", *Engineering Fracture Mechanics*, Vol. 9, pp. 931-8.

Tenchev, R.T. and Falzon, B.G. (2007), "A correction to the analytical solution of the mixed-mode bending (MMB) problem", *Composites Science and Technology*, Vol. 67, pp. 662-8.

Turon, A., D'avila, C.G., Camanho, P.P. and Costa, J. (2007), "An engineering solution for using coarse meshes in the simulation of delamination with cohesive zone models", *Engineering Fracture Mechanics*, Vol. 74 No. 10, pp. 1665-82.

Warrior, N.A., Pickett, A.K. and Lourenço, N.S.F. (2003), *Mixed-mode Delamination – Experimental and Numerical Studies*, Vol. 39, Blackwell, Oxford, pp. 153-9.

Appendix

The constitutive relations of the interface for the three modes can be expressed as follows (Camanho *et al.*, 2001; Dávila *et al.*, 2001).

No damage

$$\underline{\sigma} = \begin{bmatrix} K^{I} & 0 & 0 \\ 0 & K^{II} & 0 \\ 0 & 0 & K^{III} \end{bmatrix} \underline{\delta} = \underline{\underline{C}}\,\underline{\delta} \quad for \quad \delta_i^* \leq \delta_i \quad i = 1,2,3 \tag{18}$$

Softening

$$\underline{\sigma} = \left(\underline{\underline{I}} - \begin{bmatrix} \frac{\delta_1(\delta_1^* - \delta_{C1})}{\delta_1^*(\delta_{\max 1} - \delta_{C1})} & 0 & 0 \\ 0 & \frac{\delta_2(\delta_2^* - \delta_{C2})}{\delta_2^*(\delta_{\max 2} - \delta_{C2})} & 0 \\ 0 & 0 & \frac{\delta_3(\delta_3^* - \delta_{C3})}{\delta_3^*(\delta_{\max 3} - \delta_{C3})} \end{bmatrix} \right) \underline{\underline{C}}\,\underline{\delta} = \left(\underline{\underline{I}} - \underline{\underline{D}}\right)\underline{\underline{C}}\,\underline{\delta} \tag{19}$$

$$for\ \delta_{Ci} < \delta_i^* < \delta_i \quad i = 1,2,3$$

Damage

$$\underline{\sigma} = 0 \quad for\ \delta_i^* \leq \delta_i \quad i = 1,2,3 \tag{20}$$

where $\underline{\sigma} = \{\tau_{13} \ \ \tau_{23} \ \ \sigma_{33}\}^T$, $\underline{\delta} = \{\delta_1 \ \ \delta_2 \ \ \delta_3\}^T$, $\underline{\underline{I}}$ is the identity matrix, $\underline{\underline{C}}$ is the undamaged constitutive matrix and $\underline{\underline{D}}$ is the damaged one.

δ_i^* are the maximum relative displacements defined as:

$$\delta_1^* = \max\left\{\delta_1^*, |\delta_1|\right\} \quad \text{mode II}$$

$$\delta_2^* = \max\left\{\delta_2^*, |\delta_2|\right\} \quad \text{mode III}$$

$$\delta_3^* = \max\left\{\delta_3^*, \delta_3\right\} \quad \text{mode I}$$

The element stiffness matrix can be derived from the integral over the area of the element:

$$\underline{\underline{K}}_{elem} = \int_A \underline{\underline{B}}^T \left[\left(\underline{\underline{I}} - \underline{\underline{D}} \right) \underline{\underline{C}} \right] \underline{\underline{B}} dA \tag{21}$$

where $\underline{\underline{B}}$ is the matrix relating the element's degree of freedom $\underline{\underline{U}}$ to the relative displacements between the top and the bottom interfaces:

$$\begin{Bmatrix} \delta_1 \\ \delta_2 \\ \delta_3 \end{Bmatrix} = \begin{Bmatrix} u \\ v \\ w \end{Bmatrix}_{top} - \begin{Bmatrix} u \\ v \\ w \end{Bmatrix}_{bottom} = \underline{\underline{BU}} \tag{22}$$

Corresponding author
Luca Lampani can be contacted at: luca.lampani@uniroma1.it

This article has been cited by:

1. Kyungmok Kim, Jean Geringer, Bernard Forest. 2013. Fracture simulation for zirconia toughened alumina microstructure. *Engineering Computations* **30**:5, 648-664. [Abstract] [Full Text] [PDF]
2. Wei He, Zhidong Guan, Xing Li, Debo Liu. 2013. Prediction of permanent indentation due to impact on laminated composites based on an elasto-plastic model incorporating fiber failure. *Composite Structures* **96**, 232-242. [CrossRef]